

Tracing Russian VX to its synthetic routes by multivariate statistic of chemical attribution signatures

K. H. Holmgren, C. A. Valdez, R. Magnusson, A. K. Vu, S. Lindberg, A. M. Williams, A. Alcaraz, C. Astot, S. Hok, R. Norlin

September 6, 2017

Talanta

Disclaimer

This document was prepared as an account of work sponsored by an agency of the United States government. Neither the United States government nor Lawrence Livermore National Security, LLC, nor any of their employees makes any warranty, expressed or implied, or assumes any legal liability or responsibility for the accuracy, completeness, or usefulness of any information, apparatus, product, or process disclosed, or represents that its use would not infringe privately owned rights. Reference herein to any specific commercial product, process, or service by trade name, trademark, manufacturer, or otherwise does not necessarily constitute or imply its endorsement, recommendation, or favoring by the United States government or Lawrence Livermore National Security, LLC. The views and opinions of authors expressed herein do not necessarily state or reflect those of the United States government or Lawrence Livermore National Security, LLC, and shall not be used for advertising or product endorsement purposes.

Part 1: Tracing Russian VX to its synthetic routes by multivariate statistics of chemical attribution signatures

Karin Höjer Holmgren^a, Carlos A. Valdez^b, Roger Magnusson^a, Alexander K. Vu^b, Sandra Lindberg^a, Audrey M. Williams^b, Armando Alcaraz^b, Crister Åstot^a, Saphon Hok^{b,*} and Rikard Norlin^{a,*}

^aThe Swedish Defence Research Agency, FOI CBRN Defence and Security, SE-901 82 Umeå, Sweden ^bForensic Science Center, Lawrence Livermore National Laboratory, 7000 East Avenue L-091, Livermore, California 94550, United States

This work is supported by the Swedish Civil Contingencies Agency under Contract 2014-5170 and the Department of Homeland Security, Science and Technology Directorate - Homeland Security Advanced Research Projects Agency - Chemical and Biological Division under Contract # HSHQPM-10-X-00014 and HSHQPM-11-X-00247.

Abstract

Chemical attribution signatures (CAS) associated with different synthetic routes used for the production of Russian VX (VR) were identified. The goal of the study was to retrospectively determine the production method employed for an unknown VR sample. Six different production methods were evaluated, carefully chosen to include established synthetic routes used in the past for large scale production of the agent, routes involving general phosphorus-sulfur chemistry pathways leading to the agent, and routes whose main characteristic is their innate simplicity in execution. Two laboratories worked in parallel and synthesized a total of 37 batches of VR via the six synthetic routes following predefined synthesis protocols. The chemical composition of impurities and byproducts in each route was analyzed by GC/MS-EI and 49 potential CAS were recognized as important markers in distinguishing these routes using Principal Component Analysis (PCA). The 49 potential CAS included expected species based on knowledge of reaction conditions and pathways but also several novel compounds that were fully identified and characterized by a combined analysis that included MS-CI, MS-EI and HR-MS. The CAS profiles of the calibration set were then analyzed using partial least squares discriminant analysis (PLS-DA) and a cross validated model was constructed. The model allowed the correct classification of an external test set without any misclassifications, demonstrating the utility of this methodology for attributing VR samples to a particular production method. This work is part one of a three-part series in this Forensic VSI issue of a Sweden-United States collaborative effort towards the understanding of the CAS of VR in diverse batches and matrices. This part focuses on the CAS in synthesized batches of crude VR and in the following two parts of the series the influence of food matrices on the CAS profiles are investigated.

Keywords:

Chemical attribution signatures, Russian VX, Chemical Warfare Agents, Impurity profiling, Forensics, PLS-DA

Abbreviations:

CWA = Chemical warfare agent
CWC = Chemical weapons convention
CAS = Chemical attribution signatures
OPCW = Organization for the Prohibition of Chemical Weapons
PLS-DA = Partial least squares – discriminant analysis
PCA = Principal component analysis
PC = Principal component
VR = Russian VX

*Corresponding authors

E-mail addresses: rikard.norlin@foi.se (R. Norlin), hok2@llnl.gov (S. Hok)

1. Introduction

The use of chemical warfare agents (CWA) for acts of terrorism is a demanding issue of current relevance to society. A recent example is the assassination of an individual at the international airport in Kuala Lumpur, Malaysia, by means of the nerve agent VX [1]. The continuous reports of chemical attacks in Syria are further evidence that analytical science targeted at CWA identification and attribution can provide forensic value to this field [2]. Another indicator is the fact that the Organization of the Prohibition of Chemical Weapons (OPCW) has encouraged an increase of the scientific input on CWA forensics by the Member States [3]. In armed conflicts between countries, which historically has been an arena of chemical weapon use, there is little need for forensic information since the identity of the perpetrator of such an attack often is known from the start. However, in today's asymmetrical conflicts and terrorist acts involving CWAs against civilian targets forcibly raise important questions such as the identity of the perpetrator, the location for production of the given CWA and the method for its manufacture.

Chemical attribution profiling of confiscated material or samples collected at a crime scene where a CWA has been used is bound to provide important forensic information to contribute to finding answers to the questions raised. The profiling is based on unique composition of chemical attribution signatures (CAS) that originate during the manufacture of the CWA and consists of reaction byproducts, residual starting materials and other chemical markers specific to a synthetic pathway [4] [5]. CAS of chemical warfare agents are yet to achieve the high degree of development and characterization exhibited by those in the field of illicit drugs (e.q. amphetamine) [6]. Partial responsibility for this underdevelopment in the field of CWA forensics can be attributed to the fact that only small quantities of authentic samples are available for research and the complicated nature of handling and analyzing highly toxic chemicals that require special laboratory setups and regulatory approvals. Forensic investigation of CWA has been described in the literature [7] [8] [9] [10] [11] [12] [13] [14] [15] [16] [17] [18], however, no forensic analysis on the chemical attribution for the production of Russian VX (VR) is to our knowledge yet published. Prior studies of VR have focused on chemical verification analysis, i.e. aiming to prove the use or presence of the compound [19] [20] [21] [22]. The choice of VR as a model substance, out of the numerous VX-analogues covered by the chemical weapons convention, was motivated by the lack of characterization of this specific substance.

In the present study, VR (Fig. 1) was produced in parallel by two laboratories using six different synthesis routes that were carefully selected to cover the broadest possible range of production methodology for this material. All VR batches were exchanged and then analyzed separately by both laboratories for chemical composition of impurities and byproducts using Gas Chromatography-Mass Spectrometry (GC/MS). Based on the accumulated data, CAS profiles were extracted and modeled employing PLS-DA with the goal of attribution of VR batches to their synthetic origin (*i.e.* route). The profiling methodology described herein was undertaken with the goal of establishing it as a general approach for chemical forensic analysis to allow implementation at most analytical laboratories. This work is part one of a three-part series in this Forensic VSI issue of a Sweden-United States collaborative effort towards the understanding of the chemical attribution signatures of VR in diverse batches and matrices. This part focuses on the CAS in synthesized batches of crude VR and in the following two parts of the series the influence of food matrices on the CAS profiles are investigated [23] [24].

2. Material and method

2.1. Safety

All nerve agents, VR included, are highly toxic compounds. Appropriate protective measures must be taken in order to ensure that neither personnel nor the environment come into contact with these chemicals. All labware that has come in contact with VR must be thoroughly decontaminated (e.g. bleach decontamination) after use and the waste disposed off properly. The synthesis of CWAs is restricted by international agreements (Chemical Weapons Convention) and if the appropriate authorizations are not in place the work will be considered criminal.

2.2. Study design

VR was synthesized using six different production methods and then analyzed for CAS using GC/MS. Each synthesis was performed at two separate laboratories with at least two replicates per laboratory, except route 2. Samples from individual batches as well as the raw data from the analysis of the samples were exchanged between the laboratories giving four combinations of data (*i.e.* VR produced at Lawrence Livermore National Laboratory (LLNL) and analyzed at LLNL, VR produced at LLNL and analyzed at Swedish Defence Research Agency (FOI), VR produced at FOI and analyzed at FOI and analyzed at LLNL). All routes do not have all four combinations of the data (Table 1). Based on GC/MS data, CAS profiles were extracted and modeled using PLS-DA with the aim to link VR samples to their synthetic route of origin.

2.3. Synthesis

In order to minimize variation introduced by deviations in the chemicals employed for the synthetic routes, all chemicals (e.g. starting materials, reagents and solvents) were procured from Sigma Aldrich by both laboratories where possible. The same article number was used by both laboratories when ordering chemicals to ensure the same quality. In order to minimize variations among the synthetic routes arising from the laboratories carrying them out, identical preparation protocols were established and agreed upon. Important reaction features such as temperatures, reaction times, solvents and reagents were standardized in order to prevent the unavoidable generation of variability when comparing samples arising from a given synthetic route.

A number of factors were taken into consideration when deciding which production methods for VR to evaluate. Routes that historically have been used for large scale production of VR were immediately included in our overall assessment. In addition, routes that yield the nerve agent using steps involving general phosphorus-sulfur chemistry transformations were included in this study as these represent ways that perpetrators possessing limited resources or chemistry background may use. In the end, it was concluded that six routes (Fig. 2) would adequately cover the different production methods for VR. As outlined in Figure 2, all the routes begin with commercially available phosphorus-containing starting materials, rather than elemental phosphorus, as this represents the most likely manner in which the nerve agent will be synthesized. Each route comprised two to four different and subsequent chemical reactions or chemical transformations. No complete isolation of the intermediates were performed, only fairly simple purifications such as extractions etc. were achieved. The conversion of the intermediates in each individual reaction step were estimated from NMR spectra and GC-MS chromatograms in order to facilitate the calculation of the amounts of reagent needed for the following reactions. NMR was not used for identification of CAS.

A graphic presentation of the main starting materials of the six synthetic pathways is presented in Fig. 2. Only chemical precursors listed by the OPCW and isobutyl alcohol have been included in the figure as these compounds are known precursors of VR and information on their use for this purpose is available in the open literature [25]. Reaction details such as solvents, temperatures, reagent stoichiometry and yields that are important for VR production have deliberately been omitted in

order to prevent their unlawful employment and hinder proliferation. For reaction details please contact the authors for guidance and associated references. The number of reagents used for each route and the number of steps in each route have been added in an effort to describe the complexity of the productions.

In total, 37 batches of VR were synthesized at the two laboratories by several chemists. Four of these batches were produced following Route 1, three following Route 2, six following Route 3, and eight each following Routes 4-6.

2.4. Sample preparation

Samples were prepared from each individual synthesis step but only samples arising from the final synthetic step, the one yielding VR, were used in the profiling of CAS and subsequently in the PLS-DA predictions (Table 1). The remaining samples were used to determine the conversion of intermediates and to track the origin of certain CASs. Samples were prepared by withdrawing 2 μ L of the reaction mixture and diluting it to 1000 μ g/mL with dichloromethane (DCM, Supra Solv, Merck, Damstadt, Germany). From these, dilutions to 100 μ g/mL (DCM) samples were performed. The same lot of DCM was used for dilution of all samples within each laboratory. An aliquot of each 1000 μ g/mL sample was also derivatized for analysis of polar compounds as follows: 50 μ L sample was added to a mixture of 395 μ L DCM and 50 μ L of BSTFA ((N,O-bis(trimethylsilyl)trifluoroacetamide) + 1% TMCS (trimethylchlorosilane)) (Thermo Scientific, Bellefonte, PA, USA), then 5 μ L of a derivatization control compound (4-Tetrahydrothiopyranyl- d_3 -methylphosphonic acid, 1000 μ g/mL) was added. The derivatization was conducted at 60 °C for 60 min. NMR samples were prepared by withdrawing 2 μ L of the reaction mixture and diluting it to 1000 μ g/mL using CDCl₃ or D₂O. Samples were stored in the dark at -20 °C until analysis. The exchanged samples were enclosed in cooling blocks during the entire transport.

2.5. Chemical analysis

The same type of instrument, column and conditions for GC/MS analysis were used both at FOI and at LLNL. Each sample was analyzed using GC/MS in both electron impact (EI) mode and chemical ionization (CI) mode. Analysis in EI mode was performed using an Agilent 7890A/6890 GC equipped with a HP-5MS column (30 m long, 0.25 mm id, 0.25 μ m film thickness, Agilent Technologies). A 1 μ L aliquot of sample was introduced by splitless injection at 250 °C, with Helium as carrier gas at a constant flow of 1.0 mL/min. The column oven started at 40 °C for 1 min, followed by a 10 °C/min increase to 300 °C and hold at 300 °C for 5 min giving a runtime of 32 min. The mass spectrometer (Agilent 5975C/5973 MSD) scanned 29-500 m/z at a speed of 3.08 scan/s. The temperature of the transfer line, ion source and quadrupole were set at 280 °C, 230 °C and 150 °C, respectively. An Agilent 6890 GC/Agilent 5973 MS was used for the GC/MS-CI analysis with isobutane or ammonia as CI gas in positive mode using a scan range of 60-550 m/z at a scan speed of 3.03 scan/s. The ion source was set at 300 °C and the quadrupole at 150 °C. All other settings were the same as in EI mode.

A quality control (QC) sample, consisting of eight compounds of different properties and a hydrocarbon series (C_8 - C_{28}) dissolved in DCM, was run in the beginning of each sample sequence as well as after approximately every 10th sample. The QC samples were used for two purposes; to monitor the condition of the GC/MS system and to perform a retention index calibration. Furthermore, a blank analysis (DCM or DCM+BSTFA) preceded each sample during the analysis.

One 1000 μ g/mL sample from each route was analyzed using a GC-TOFMS-EI employing a Leco Pegasus 4D coupled to an Agilent GC 6890 using similar settings as described above [26]. Data was

acquired within the mass range of 38-500 m/z. Mass calibration measurements yielded a resolution of 0.1 to 0.3 ppm. The GC-TOF-MS data was used for CAS identification.

NMR analysis were performed using a Bruker Avance II 500 MHz NMR spectrometer. 1 H-NMR and 31 P-NMR spectra were recorded using standard parameter files from Bruker. Tetramethylsilane was used as a reference and the samples were analyzed in CDCl₃ or D₂O

2.6. Identification of CAS

CAS were identified by extracting mass spectra from chromatographic peaks using Automatic Mass Spectral Deconvolution and Identification Software (AMDIS, version 2.70, National Institute of Standards and Technology, NIST, Gaithersburg, MD, USA) and matched against mass spectra libraries (NIST 11 Version 2.0g and OPCW Central Analytical Database (OCAD ver. 19). These tentative identifications were supported by the use of retention indices calculated by AMDIS for each compound and by molecular weights determined from GC/MS-CI data. Mass spectra for compounds not found in mass spectra libraries were manually interpreted with the aid of previously published data [27] [28] [29]. GC/MS analysis of 1000 µg/mL samples were used to improve the identification in cases where the 100 µg/mL samples gave unclear results, for instance if MS-CI data had low signalto-noise ratio for a certain peak. In addition, further analysis on CAS was accomplished by studying samples arising from the previous synthesis steps, an approach that contributed to CAS tracking and to understand were in the process the different CAS were formed. GC/HRMS data were also produced for identification of selected compounds. The combined use of all available information mass spectrum, molecular weight, retention index and synthetic pathway origin – resulted in tentative CAS identities assessed with relatively high degree of certainty (see supporting material). Where available, reference substances were used to provide unambiguous identification.

2.7. Data processing

GC/MS-EI raw data from 57 samples (the 100 µg/mL samples), see Table 1, were processed to generate a peak table. The table includes samples produced at both LLNL and FOI that were analyzed independently at each location. AMDIS was used in conjunction with a target library consisting of spectra, retention indices (RI), and tentative identities (if known) for all CAS with chromatographic peaks exceeding 0.5 % of total area. All chromatograms were analyzed by AMDIS for automated identification of target peaks and the automatic calculation of corresponding peak areas. AMDIS was used to search the target library retention indices for matching CAS to the chromatographic peaks, minimum match factor was set to 50-70. For compounds displaying a high match factor (Net match factor \geq 90) and correct retention index (\pm 20 units) the area of the peak was transferred to a worksheet in Excel. Peaks with RI close to ± 20 units and match factor between 70 and 90 were checked manually before deciding whether to include them in the worksheet or not. During data processing, no threshold for peak area was set. Hence, for a particular compound, peak areas smaller than 0.5 % were included if the peak area of this compound exceeded 0.5 % for at least one of the samples. The resulting peak table contained one row for each sample and one column for each CAS. The peak areas for each sample in the peak table were normalized so that the total area for all peaks in one sample equaled 100 %. To evaluate if the polar CAS (TMS-derivatized compounds) incorporated valuable information to the CAS profiles, one additional peak table was created for each sample in which the peak areas of the polar CAS were added in the same row as the corresponding underivatized sample. Then, the peak areas for each row in this polar CAS included peak table were normalized so that the total area for all peaks in one row equaled 100 %.

2.8. Multivariate analysis

Multivariate statistic evaluation of the normalized peak table were performed using the software SIMCA 13.0.2.0 (Sartorius Stedim Biotech). Two different multivariate statistical approaches were used: PCA was used to get an overview of the variation in the dataset, while PLS-DA [30] was used in the classification of the synthetic routes. All processed data were mean-centered and different types of scaling and transformation of the data were evaluated. Applying a logarithmic transformation, log (X+0.01), in order to normalize the data distribution was found to produce best results for our data. Using this transformation, the performance of unit variance (UV)-scaling proved to perform best on our data for PCA models, and the combination based on log-transformation/Pareto was chosen for PLS-DA modelling.

3. Results and Discussion

3.1. Synthesis

VR was successfully produced by all the studied routes with conversion ranging between approximately 5 to 80%. In addition to VR, a large number of byproducts and impurities were found in the reaction mixtures. Each synthesis route was performed in at least two replicates by each laboratory generating 37 unique batches of VR to sample. Over all more than 100 individual synthesis steps were performed which all, in various degree, left traces in the VR batches produced.

3.2. Chemical analysis and identification of CAS

A large number of impurities and byproducts from synthesis was observed in the samples (Fig. 3, supporting material). As can be seen in the figure, it is difficult to use visual interpretation in order to link a certain CAS profile to the correct synthesis route. All of the VR production routes involve several individual reaction steps, increasing the possibility for generating a vast number of CAS. In order to process the information contained in the samples, a relatively high threshold was set in order to reduce the number of CAS to a manageable quantity. Most of the CAS had a large variation of their relative intensities between samples, even within the intralab replicates. In such cases it was often found that the difference between samples originating from the two laboratories was even greater. For example, Table 2 shows the normalized peak areas of four individual CAS from four samples produced by the same route (including replicates) and synthesized at both labs. Three interesting observations should be emphasized; first, the normalized areas of diisobutyl methylphosphonate displayed a large difference between the two replicates synthesized at FOI, while the replicates synthesized at LLNL showed more similarity, indicating that the variation of a single CAS between replicates is often difficult to interpret. Secondly, there were pronounced differences between the laboratories, for example, the normalized areas for O-isobutyl O-[2-(diethylamino)ethyl] methylphosphonothioate were above 44.5 for the LLNL synthesis replicates but found to be below 4.8 for the FOI synthesis replicates indicating laboratory specific CAS profiles. Thirdly, the normalized areas for these CAS remained relatively constant after shipping the samples overseas for a second analysis indicating stability of those specific CAS and that the performance of the GC-MS analysis was similar between the laboratories. The benefit of performing the study at more than one laboratory to cover inter-lab-variation was apparent when interpreting the data described above.

Taking all data into account, most CAS were present in a majority of the routes and the number of CAS unique for a single route were few. In total, 49 different CAS were identified based on the chemical analyses of all routes. Out of these compounds, 21 were identified based on hits in instrument spectral libraries, 17 compounds were tentatively identified by spectra interpretation, 5 of the CAS were verified by the use of reference substances, and 11 of the compounds remain unidentified. When the samples were derivatized prior to GC-MS analysis, an additional number of

18 polar compounds (e.g. phosphonic acids and phosphonothioic acids) were identified as their TMS derivatives [31] [32]. However, there were indications that the derivatization of VX samples was prone to produce artifacts not present in the original samples, implying a risk of adding artificial CAS to the process [33]. Identification of all individual CAS would have been an optimal scenario, however this is not within the scope of the study. It is important to emphasize that an identified structure is not required for inclusion of a CAS in the multivariate modeling approach used in this study. However, the known CAS identities allowed a more in depth investigation of the profiles. With an established chemical identity it is possible to assess the origin of an identified CAS via a thorough analysis of the specific synthetic route it derived from, thus placing additional input for the interpretation and validity of the model.

The identified CAS were phosphonates, phosphonothioates, analogues of VR, pyrophosphonates and diethylamine derivatives. Two chemicals, isobutyl methylphosphonic acid and isobutyl methylphosphonothionic acid, were present in all samples. In addition, methyl phosphonic acid and diisobutyl methylphosphonate were found in almost all samples along with pyro phosphonate-based species that were present in samples from all routes but not in all replicates. The CAS are often analogues of the same type of compounds and determining their exact structure via interpretation of mass spectra can then become a daunting task. The MS-EI fragmentation patterns among the VR analogues showed a high degree of similarity compared to VR but their retention indices, and molecular weights, and/or molecular formula deviated from VR allowing their differentiation. A few of these analogues were preliminary identified as O-isobutyl- O-[2-(diethylamino)ethyl] methylphosphonothioate and O-isobutyl- S-[2-diethylaminoethyl] methylphosphonodithioate (Fig. 4).

3.3. Route classification

The CAS profiles of all 57 underivatized samples from the six synthetic routes were included in a PCAmodel to get an overview of the data. The PCA-model with 57 observations and 49 variables (CAS) required seven significant principal components to explain 82 % of the data variance ($R^2X = 0.82$, $Q^2 =$ 0.49). The use of Pareto scaling or no scaling (only mean centering) of the variables gave similar results in terms of cross validation ($Q^2 = 0.46$ using Pareto and $Q^2 = 0.45$ using centering). The score plots revealed no evident outliers and therefore all samples were included in the building of the model. Furthermore, the samples from each route clustered in separate groups. Since clustering of the routes was observed in the PCA score plot already using the 57 underivatized samples, these were the samples primarily used for construction of the PLS-DA prediction model (M1, Table 3). This approach reduces the analytical complexity and amount of data to be processed, hence facilitating the reproduction at most analytical laboratories. In order to evaluate if the derivatized samples contained valuable information to the CAS profiles, data of the polar CAS (TMS-derivatized compounds) were incorporated in a second PLS-DA model (M2, Table 3). M2 describes the variation between the six routes slightly better with a small increase in both R²Y and Q². The amount of work for generating a peak table with both TMS and non TMS data is substantially increased and the performance of the prediction of the test set samples using M2 did not increase when compared to the original PLS-DA model (data not shown). Thus, the addition of polar CAS such as methylphosphonic acid, methylphosphonothioic acid, isobutyl methylphosphonic acid, isobutyl methylphosphonothioic acid, and isobutyl S-(2-diethylaminoethyl) methylphosphonothioic acid in the predictions was considered superfluous. Furthermore these chemicals are common degradation products of VR and are likely to exist in most VR samples.

A third model (M3) was built using the derivatized and underivatized data where the 20 least important CAS, as estimated by the model, were removed from M2 to evaluate if this could be done without affecting the model's predictive ability. Among the 20 compounds removed were both

derivatized and underivatized CAS. The results showed that the predictive ability of the model was efficient in the reduced version of M2. The reduction of up to 20 CAS proved that the route classification was not particularly sensitive to removal of some individual compounds and that some noise could be removed by variable reduction. However, the removal of even more CAS reduced the predictive ability significantly, indicating that approximately 45 CAS were needed to retain the performance of the route classification. Since there are a number of unidentified compounds among the CAS it is difficult to assess the importance of the individual CAS removed or not, why we recommend that as many CAS as possible are used in the modeling and in the predictions of routes.

M1 with all 57 underivatized samples resulted in a 10 principal component (PC) model with a cross validated predictive ability $Q^2 = 0.85$ and total explained variance $R^2X = 0.89$. The six routes were all well described by the model with individual R^2Y values of 0.9 or higher and Q^2 values above 0.8. The score plots of the four dominant PC's (Fig. 5) separated samples from each route from the other routes. Samples from routes 4 and 5 separated well in the score plot of PC 1 vs PC 2(Fig. 5, top), whereas separation of routes 1, 2, 3 and 6 samples are seen in score plot of PC 3 vs PC 4 (Fig. 5, bottom). Samples from routes 3, 4 and 6 displayed small variation and clustered tightly in well-defined groups whilst samples from routes 1, 2 and 5 were more widely spread in the score plot. This is consistent with the observations made during synthesis where routes 3, 4 and 6 were robust and more straight-forward to perform. This compared to routes 1, 2 and 5 which represent more complex chemical conditions.

In order to illustrate the variability between replicates in more detail and the different traits of CAS profiles of different routes, a reduced PCA model was built on samples from only routes 1 and 3 (3PCs, $R^2 = 0.83$ and $Q^2 = 0.64$). In the score plot of the two first PCs (Fig. 6), samples from route 3 display small variations between replicates, both within the same laboratory and between the laboratories. In addition, the reanalyzed samples that were transported overseas are all clustered tightly in one distinct group. Hence, the results indicate that the synthesis of VR according to route 3 is fairly reproducible and the CAS profiles seem to be stable. In contrast, the variation between samples from route 1 is much larger. The four synthesis replicates analyzed directly at the laboratory of origin deviate both within and between laboratories. The variation was found to be linked to both the synthesis replicates and the effect brought upon by aging and transport of samples. Hence the synthesis of route 1 creates batches displaying greatly diverging CAS profiles, both within as well as between laboratories, and the profiles are not stable over time when transported and resubjected to analysis. It is important to have enough samples to cover the variation in CAS profiles within a given route and the associated variation brought upon the sample by other factors in order for the model to work as efficiently as possible. Ultimately, an ideal model should be based on CAS that are stable over time or built on a model that can incorporate the degradation of these species over time.

PLS-DA regression coefficients were used to evaluate the importance of individual CAS for attribution of samples to specific synthesis routes and to get an overview of how the CAS profiles were composed (Fig. 7). Each route possesses their individual set of key CAS (*i.e.* significantly correlated), that differentiate it from others. For example, the coefficient plots illustrate that compound 2(N,N-diethylaminoethyl-2-chloride), shown as number 2 in Fig. 7, is positively correlated to samples from route 5 and route 6 and negatively correlated to samples from route 3 and route 4, whereas being insignificant for samples of route 1 and route 2. Route 2 does not show any individually significant CAS. Coefficient plots facilitated the evaluation of the importance of individual CAS for each route, however, the signatures positively correlated to a route were not necessarily unique for that route and could still be present in other routes. By visual interpretation of the regression coefficients plots

it is evident that CAS contributes heterogeneously to the CAS profiles and that most CAS are important for differentiating between routes.

3.4. Validation with external test set

The validation of the PLS-DA model was performed using an external test set. The use of an external test set for validation requires that the samples included in the test set are not used for construction of the PLS-DA model and hence can be regarded as unknown samples. When the routes of the test set samples are predicted, the performance of the model can be assessed based on the correspondence between predicted and true values. Ideally, a sample that belongs to a specific class (in this case route) would have a predicted value of 1 for that specific class and members of other classes would get a predicted value of 0. The deviation from these values for the test set samples give a measure of the model's predictive ability. A test set was selected out of the 57 samples, consisting of 11 samples. The test set was chosen to include two replicates from each route (one FOI sample and one LLNL sample) except for route 2 from which only one replicate was selected since only three replicates were available from that route (see supporting material).

A PLS-DA model was calculated based on the remaining 46 samples (10 PCs, $R^2Y = 0.94$ and $Q^2 = 0.81$) and this model was used for route classifications of the samples in the test set. As shown in Table 4 the model correctly assigned the routes for all 11 samples in the test set (predicted values close to 1). The classification of sample 2 (R11UU) to route 1 deviated from a predicted value of 1 but route 1 was still by far the best prediction for that sample (all other routes having predicted values close to 0). The difficulty to assign this sample could be explained by the greater sample-to-sample variability seen for route 1. Furthermore, no test samples were misclassified (all values were close to 0 when not belonging to the class).

All samples produced within the study were classified to correct routes using the methodology presented in this work, thus demonstrating the strength of the developed approach. Nonetheless, the model developed in this study is based on a limited amount of samples and the development of a validated forensic method would require a model based on data involving more VR samples. More VR samples of different origin could be included to increase the resolving power of the model. The design of this study was established in order to narrow its scope to a reasonable size. The aim was to ensure that the variability of CAS profiles originated mainly from production methods rather than from specific solvents, reagents, storage, environmental factors, etc. It is important to note that in order to strengthen the model described herein, more refined studies on the synthesis route attribution of VR would merit additional routes and elements that could not be covered in this study. Consequently, if the same analytical procedures described in this study are employed during the analysis, the model could easily be expanded to include more samples and thus become more refined.

4. Conclusions

VR was produced by six synthetic routes and all samples of the test set were correctly classified according to the production routs. The key conclusion is that most CAS within the samples are relevant for classification and contribute to various degrees to the profiling. By using a large number of CAS the model is not as vulnerable to changes of individual CAS as a prediction of routes based only on one or a few specific CAS would be. The collaboration between the laboratories added extra value in the identification of relevant synthesis pathways and in the identification of unknown CAS. However, the collaboration has been crucial in obtaining inter-lab cross validation achieved by exchanging samples as well as exchanging analyzed data between the laboratories and to combine all of the data in one model.

5. Acknowledgement

Financial support from the Swedish Civil Contingencies Agency (under Contract 2014-5170) and the Department of Homeland Security, Science and Technology Directorate, Chemical Forensic Program (under Contract # HSHQPM-10-X-00014 and HSHQPM-11-X-00247), United States is gratefully acknowledged. Lawrence Livermore National Laboratory is operated by Lawrence Livermore National Security, LLC, for the U.S. Department of Energy, National Nuclear Security Administration under Contract DE-AC52-07NA27344.

Annexes

1. Compound list

References

- [1] https://www.opcw.org/fileadmin/OPCW/EC/84/en/ec84dec08 e .pdf. [Online] 2017.
- [2] United Nations. http://www.securitycouncilreport.org/syria/. [Online]
- [3] Report of the Scientific Advisory Board's Workshop on Chemical Forensics, 24th Session of the Scientific Advisory Board(SAB), SAB-24/WP.1, 14 July 2016.
- [4] M. Mazitelli, M. Re, M. Reaves, C. Acevedo, S. Straight, J. Chipuk, A Systematic Method for the Targeted Discovery of Chemical Attribution Signatures: Application to Isopropyl Bicyclophosphate Production., Anal. Chem. 84 (2012) 6661-6671.
- [5] B. P. Mayer, A. J. DeHope, D. Mew, P. E. Spackman, A. M. Williams, Chemical attribution of fentanyl using multivariate statistical analysis of orthogonal mass spectral data, Anal. Chem. 88 (2016) 4303-4310.
- [6] M. Morelato, A. Beavis, M. Tahtouh, O. Ribaux, P. Kirkbridge, C. Roux, The use of forensic case data in intelligence-led policing: The example of drug profiling, Forensic Sci. Int. 226 (2013) 1-9.
- [7] K. H. Favela, J. A. Bohmann, W. S. Williamson, Dust as a collection media for contaminant source attribution, Forensic Sci. Int. 217 (2012) 39-49.
- [8] C. G. Fraga, G. A. P. Acosta, M. D. Crenshaw, K. Wallace, G. M. Mong, H. A. Colburn, Impurity profiling to match a nerve agent to its precursor source for chemical forensics applications, Anal. Chem. 83 (2011) 9564-9572.
- [9] C. G. Fraga, K. Bronk, B. P. Dockendorff, A. Heredia-Lagner, Organic chemical attribution signatures for the sourcing of a mustard agent and its starting materials, Anal. Chem. 88 (2016) 5406-5413.
- [10] N. S. Mirjankar, C. G. Fraga, A. J. Carman, J. J. Moran, Source attribution of cyanides using anionic impurity profiling, stable isotope ratios, trace elemental analysis and chemometrics. Anal. Chem. 88 (2016) 5406-5413.
- [11] J. Hoggard, J. Wahl, R. Synovec, G. Mong, C. G. Fraga, Impurity profiling of a chemical weapon precursor for possible forensic signatures by comprehensive two-dimensional gas chromatography/mass spectrometry and chemometrics. Anal. Chem. 82 (2010) 689-698.
- [12] C. G. Fraga, B. Clowers, R. Moore, E. Zink, Signature discovery approach for sample matching of a nerve-agent precursor using liquid chromatography-mass spectrometry, XCMS, and chemometrics, Anal. Chem. 82 (2010) 4165-4173.

- [13] C. G. Fraga, J. Wahl, S. Nunez, Profiling of volatile impurities in tetramethylenedisulfotetramine (TETS) for synthetic-route determination, Forensic science international 210 (2011) 164-169.
- [14] C. G. Fraga, L. Sego, J. Hoggard, G. Acosta, E. Viglino, J. Wahl, R. Synovec, Preliminary effects of real-world factors on the recovery and exploitation of forensic impurity profiles of a nerve-agent simulant from office media. J. Chromatography 1270 (2012) 269-282.
- [15] D. Beringer, D. Smith, V. Katona, A. Lewis, L. Hernon-Kenny, M. Crenshaw, Demonstration of spread-on peel-off consumer products for sampling surfaces contaminated with pesticides and chemical warfare agent signatures, Forensic science international 241 (2014) 7-14.
- [16] N. Mirjankar, C. G. Fraga, A. Carman, J. Moran, Source attribution of cyanides using anionic impurity profiling, stable isotope ratios, trace elemental analysis and chemometrics, Anal. Chem. 88 (2016) 1827-1834.
- [17] C. G. Fraga, K. Bronk, B. Dockendorff, A. Heredia-Langner, Organic chemical attribution signatures for the sourcing of a mustard agent and its starting materials, Anal. Chem. 88 (2016) 5406-5413.
- [18] E. Strozier, D. Mooney, D. Friedenberg, T. Klupinski, C. Triplett, Use of comprehensive two-dimensional gas chromatography with time-of-flight mass spectrometric detection and random forest pattern recognition techniques for classifying chemical threat agents and detecting chemical attribution signatures, Anal. Chem. 88 (2016) 7068-7075.
- [19] D. Carmany, A. Waltz, F. L. Hsu, B. Benton, D. Burnett, J. Gibbons, D. Noort, T. Glaros, J. Sekowski, Activity based protein profiling leads to identification of novel protein targets for nerve agent VX. Chemical Research in Toxicology 30 (2017) 1076-1084.
- [20] T. P. Mathews, M. D. Carter, D. Johnson, S. L. Isenberg, L. A. Graham, J. D. Thomas, R. C. Johnson, High-confidence qualitative identification of organophosphorus nerve agent adducts to human butyrylcholinesterase, Anal. Chem. 89 (2017) 1955-1964.
- [21] C. Montauban, A. Begos, B. Bellier, Extraction of nerve agent VX from soils, Anal. Chem. 76 (2004) 2791-2797.
- [22] M. R. Gravett, F. B. Hopkins, A. J. Self, A. J. Webb, C. M. Timperley, J. R. Riches, Fate of the chemical warfare agent O-ethyl S-[2-diisopropylaminoethyl] methylphosphonothiolate (VX) on soil following accelerant-based fire and liquid decontamination. Anal. Bioanal. Chem. 406 (2014) 5121-5135.
- [23] D. Jansson, S.W. Lindström, R. Norlin, S. Hok, A.M. Williams, C. Nilsson, C. Åstot.. Forensic attribution profiling of Russian-VX in food using Liquid Chromatography-Mass Spectrometry, Talanta This issue (2017).
- [24] Audrey M. Williams, Alexander K. Vu, Brian Mayer, Saphon Hok, Carlos Valdez, Armando Alcaraz, Extraction and Detection of Russian VX and its Chemical Attribution Signatures in Food and Environmental Matrices at LLNL, Talanta This issue (2017).
- [25] Organisation for the Prohibition of Chemical Weapons. OPCW.org/chemical-weapons-convention/annexes/annex-on-chemicals. [Online]
- [26] M. Ripszam, C. Gallampois, Å. Berglund, H. Larsson, A. Andersson, M. Tysklind, P. Haglund, Effects of predicted climatic changes on fates of organic contaminants in brackish water mesocosms, Science of The Total Environment 517 (2015) 10-21.

- [27] P.A. D'Agostino, L. R. Provost, J. Visentini, Analysis of O-Ethyl S-[2-(diisopropylamino)ethyl] methylphosphonothiolate (VX) by capillary column gas chromatography-Mass spectrometry, Journal of Chromatography 402 (1987) 221-232.
- [28] A. Bell, J. Murrell, C. M. Timperley, P. Watts, Fragmentation and reactions of two isomeric O-alkyl S-[2-dialkylamino]ethyl methylphosponothiolates studied by electrospray ionization/ion trap mass spectrometry, J. Am. Soc. Mass Spectrom. 12 (2001) 902.
- [29 D. K. Rohrbaugh, Mass spectral fragmentation of VX. s.l: Edgewood chemical Biological Center, 2008. ECBC-TR-618.
- [30] L. Eriksson et al, Multi and megavariate data analysis part I. Basic principles and applications, second revised and enlarged edition. Umeå: s.n., 2006. ISBN-13:978-91-973730-2-9.
- [31] R. M. Black, B. Muir, Derivatisation reactions in the chromatographic analysis of chemical warfare agents and their degradation products, J. Chromatogr. A. 1000 (2003) 253-281.
- [32] Y. Yang, J. A. Baker, J. R. Ward, Decontamination of chemical warfare agents, Chem. Rev. 92 (1992) 1729-1743.
- [33] Evaluation of Results, Twenty-Sixth Official OPCW Proficiency Test, Volume III, March 2010, Technical Secretariat OPCW. DRDE Report No: DRDE-VTX-26PT-EVAL-REPORT-02

FIGURE AND TABLE CAPTIONS

Figure 1. Model compound Russian VX (VR).

| Synthesis laboratory | FOI | FOI | FOI | FOI | LLNL | LLNL | LLNL | LLNL |
|---|------|-----|------|------|------|------|------|------|
| Replicate | 1 | 2 | 1 | 2 | 3 | 4 | 3 | 4 |
| Analysis laboratory | FOI | FOI | LLNL | LLNL | LLNL | LLNL | FOI | FOI |
| Diisobutyl methylphosphonate | 59.3 | 4.1 | 66.7 | 5.8 | 1.1 | 0.5 | 0.9 | 1.8 |
| O-isobutyl O-[2- (diethylamino)ethyl)] methylphosphonothioate | 0.5 | 4.8 | 0.2 | 4.5 | 62.7 | 71 | 44.5 | 51 |
| O,O-diisobutyl methylphosphonothionate | 0.9 | 0.9 | 1.7 | 1.4 | 11.2 | 8.4 | 10.8 | 7.9 |
| O-isobutyl S-(2-diethylaminoethyl) methylphosphonodithioate | 0.5 | 4.7 | n.d. | 5.6 | 0.6 | 3.0 | n.d. | n.d. |

n.d. = not detected

Table 1. The samples (100 μ L/mL GC/MS) withdrawn from the different routes R1-R6 and included in the multivariate data analysis. Samples synthesized at FOI or LLNL and analyzed at FOI or LLNL (X= Data missing).

| PLS-DA models | Variables | Observations | Components | R^2X | R ² Y | Q^2 |
|-----------------------------------|-----------|--------------|------------|--------|------------------|-------|
| | (CAS) | (samples) | | | | |
| M1. Original model | 49 | 57 | 10 | 0.89 | 0.93 | 0.85 |
| M2. Model with polar CAS included | 67 | 57 | 11 | 0.88 | 0.96 | 0.86 |
| M3. Reduced M2 model | 47 | 57 | 11 | 0.89 | 0.96 | 0.87 |

Table 2. Relative abundance (%) of four CASs in one of the routes. All four synthesis replicates are analyzed at both laboratories.

| Route | Starting material | Main building blocks | Number of chemicals and steps involved |
|-------|-----------------------------|-------------------------|--|
| 1 | O II —P—CI I CI | HO HO N | 10 Chemicals through 4 steps |
| 2 | O II —P—CI I CI | HO HO N | 10 Chemicals through 4 steps |
| 3 | O | HO HS N | 8 Chemicals through 2 steps |
| 4 | CI CI | HO CI | 12 Chemicals through 3 steps |
| 5 | CI —P CI | HO HO N | 9 Chemicals through 3 steps |
| 6 | CI CI | HO CI N | 12 Chemicals through 3 steps |

Figure 2. A graphic presentation of the main starting materials and building blocks of the six synthetic pathways.

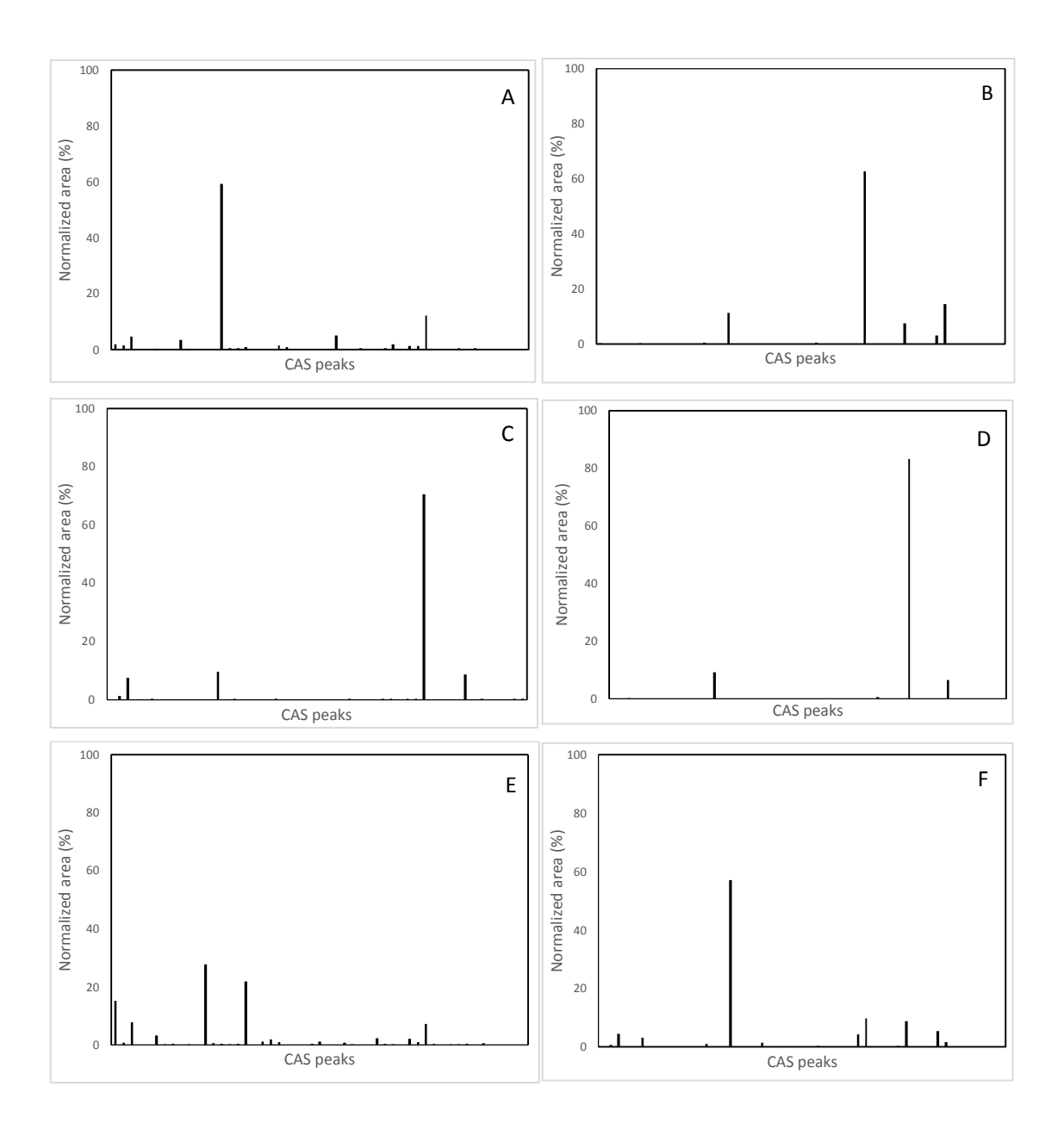


Figure 3. CAS profiles of six VR batches. Each bar represents a compound and the sum of all peak areas are normalized to 100%. The graphs represent route 1 batches synthesized at FOI (A) and at LLNL (B), route 3 batches synthesized at FOI (C) and at LLNL (D) and route 5 batches synthesized at FOI (E) and at LLNL (F).

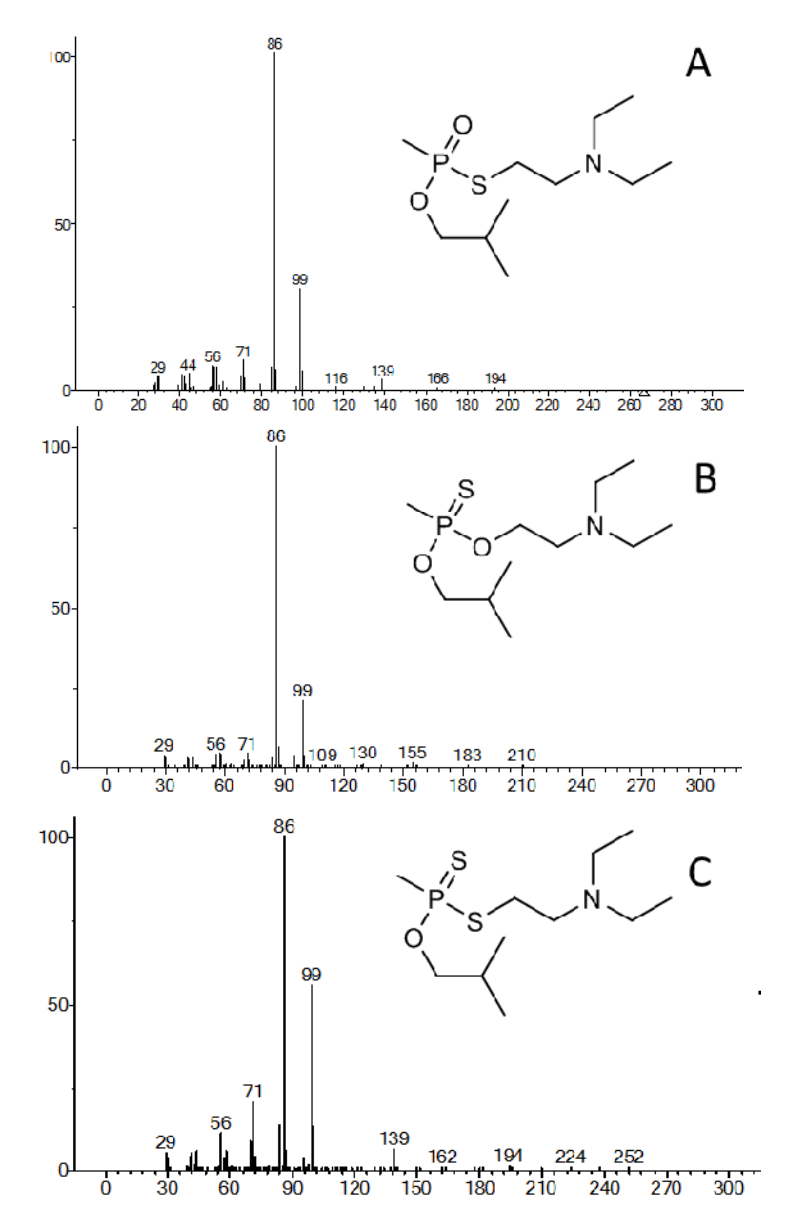


Figure 4. Mass spectra of VR and two previously not described VR-related compounds. A) VR spectrum from OCAD library (MW = 267, $C_{11}H_{26}NO_2PS$). B) Spectrum of O-isobutyl-O-[2-(diethylamino) ethyl] methylphosphonothioate (empirical data: MW = 267, $C_{11}H_{26}NO_2PS$) tentatively identified. C) Spectrum of O-isobutyl-S-[2-diethylaminoethyl] methylphosphonodithioate (empirical data: MW = 283, $C_{11}H_{26}NOPS_2$) tentatively identified.

| PLS-DA models | Variables | Observations | Components | R^2X | R ² Y | Q^2 |
|-----------------------------------|-----------|--------------|------------|--------|------------------|-------|
| | (CAS) | (samples) | | | | |
| M1. Original model | 49 | 57 | 10 | 0.89 | 0.93 | 0.85 |
| M2. Model with polar CAS included | 67 | 57 | 11 | 0.88 | 0.96 | 0.86 |
| M3. Reduced M2 model | 47 | 57 | 11 | 0.89 | 0.96 | 0.87 |

Table 3. Model performance under different settings.

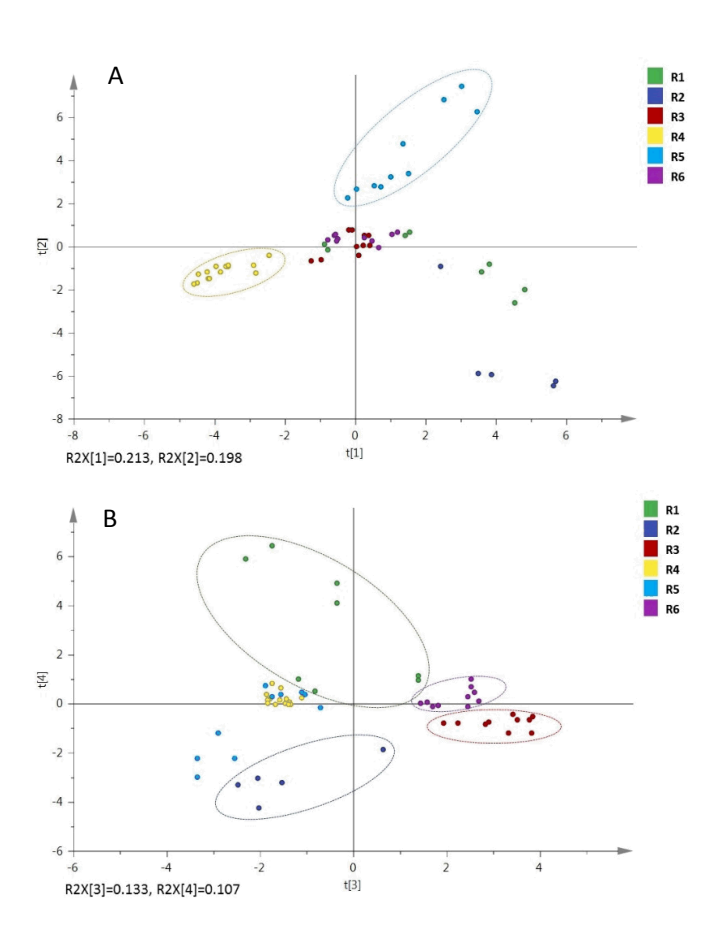


Figure 5. Score plots of the PLS-DA model (PC1 versus PC2 above, PC3 versus PC4 below).

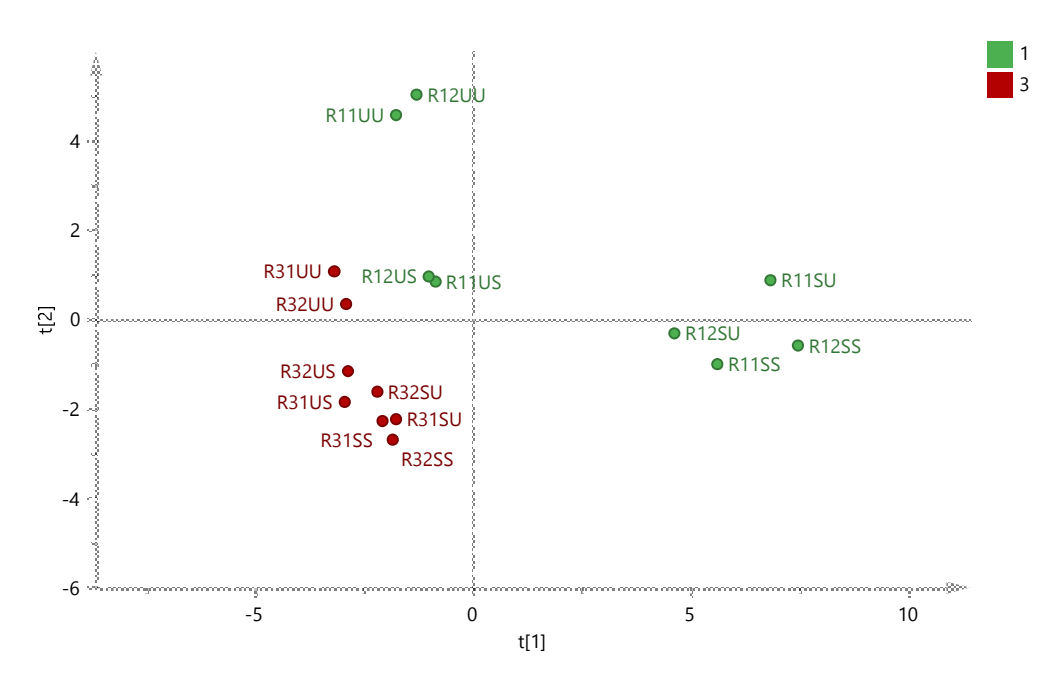


Figure 6. Score plot of PCA model based on samples from route 1 and route 3 (PC1 versus PC2). Samples are named according to route (R1 or R3), replicate (1 or 2), synthesis laboratory (U=LLNL or S=FOI) and analysis laboratory (U=LLNL or S=FOI).

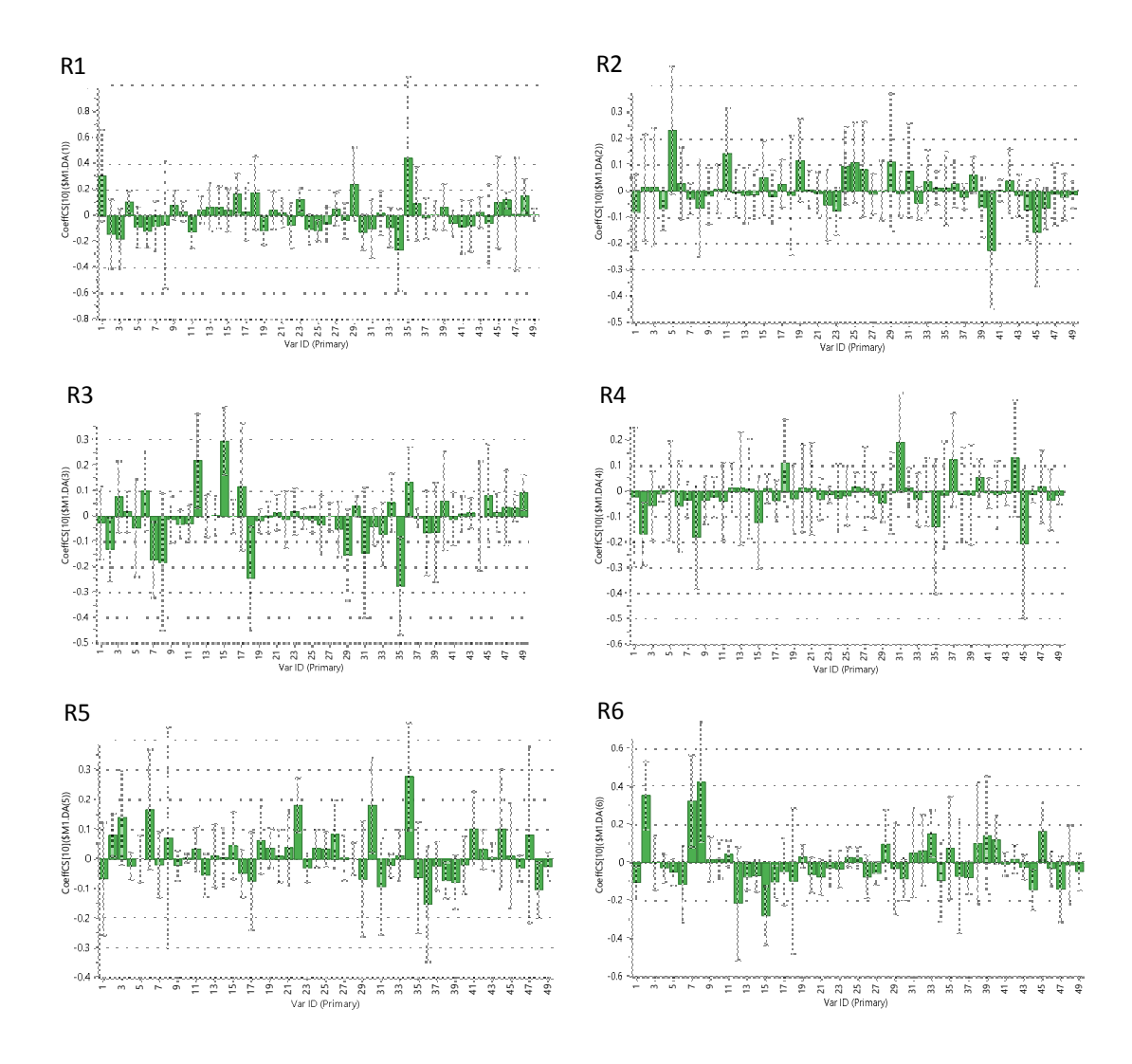


Figure 7. Coefficient plots for R1, R2, R3, R4, R5 and R6 illustrating the relative importance of some of the CAS for different routes. Compounds are numbered 1 to 49 but the numbering differs compared to supporting material.

| | R1 | R2 | R3 | R4 | R5 | R6 |
|---------------------|-------|-------|-------|-------|-------|-------|
| Test sample 1 (R1) | 1.04 | 0.01 | 0.17 | 0.08 | -0.17 | -0.13 |
| Test sample 2 (R1) | 0.64 | -0.07 | -0.11 | 0.18 | 0.13 | 0.23 |
| Test sample 3 (R2) | 0.04 | 1.05 | 0.09 | -0.13 | -0.04 | -0.01 |
| Test sample 4 (R3) | 0.01 | 0.03 | 0.77 | 0.07 | -0.02 | 0.14 |
| Test sample 5 (R3) | 0.06 | 0.05 | 1.14 | 0.03 | -0.05 | -0.23 |
| Test sample 6 (R4) | 0.02 | 0.02 | -0.04 | 1.05 | -0.07 | 0.02 |
| Test sample 7 (R4) | -0.01 | 0.06 | 0.12 | 0.92 | 0.15 | -0.23 |
| Test sample 8 (R5) | 0.22 | -0.01 | -0.02 | 0.06 | 0.99 | -0.23 |
| Test sample 9 (R5) | 0.16 | 0.04 | -0.07 | 0.00 | 0.89 | -0.03 |
| Test sample 10 (R6) | -0.04 | -0.07 | 0.35 | 0.07 | 0.00 | 0.69 |
| Test sample 11 (R6) | 0.00 | 0.07 | 0.08 | 0.00 | 0.06 | 0.79 |

Table 4. PLS-DA classification of routes for an external test set consisting of eleven samples. Classification criteria was set to: <0.35 = do not belong to the class (white), 0.35 to 0.65 = May or may not belong to the class (orange), and 0.65-1.35 = belonging to the class (green).

Graphical abstract

